True three-dimensional proximity effect correction in electron-beam lithography

Kasi Anbumony and S.-Y. Lee[a)]

Department of Electrical and Computer Engineering, Auburn University, Auburn, Alabama 36849

Proximity effect in e-beam lithography is mainly due to the "nonideal" distribution of exposure (*energy deposited* in the resist). The proximity effect correction schemes developed so far employ a two-dimensional (2D) model, i.e., exposure variation along the resist depth dimension is not considered. The exposure distribution estimated by the 2D model can be significantly different from the actual exposure distribution, especially for the nanoscale patterns. In this article, a three-dimensional (3D) correction method which uses a 3D point spread function in controlling e-beam dose distribution within each circuit feature in order to achieve a certain desired 3D remaining resist profile after development is described. The dose to be given to each region of a feature is determined based on the estimated remaining resist profile (with the emphasis on the sidewall shape) through iterations. Simulation results demonstrating the potential improvements by the 3D correction are provided. © *2006 American Vacuum Society.* [DOI: 10.1116/1.2388960]

I. INTRODUCTION

Proximity effect in e-beam lithography is mainly due to the "nonideal" distribution of exposure (*energy deposited* in the resist). There have been extensive research efforts to develop proximity effect correction methods.[1–6] While the resist is inherently three-dimensional (3D), the proximity effect correction schemes developed so far employ a two-dimensional (2D) model, i.e., exposure variation along the resist depth dimension is not considered. In other words, a 3D *point spread function* (PSF), which describes the energy deposition profile throughout the resist when a point is exposed, is not directly used in correction but usually averaged along the depth dimension to obtain a 2D PSF. Note that the 2D model is equivalent to a 3D model where all isoexposure contours (surfaces) are completely vertical to the *X-Y* plane. As previously analyzed through simulation,[7] the exposure distribution estimated by the 2D model can be significantly different from the actual exposure distribution, especially for the nanoscale patterns or structures. Accordingly, proximity effect correction based on the 2D model would not lead to the optimal result.

Another shortcoming of the conventional e-beam proximity effect correction schemes is that they consider exposure distribution only. However, the resist developing rate is not linearly proportional to exposure. Also, not all points in the resist are exposed to the developer at the same time, i.e., the developing process is sequential from the top surface of the resist toward the bottom. Therefore, the remaining resist profile after development can be significantly different from an isoexposure contour.

The main objective of this study is to investigate if and how a specified remaining resist profile can be achieved by controlling dose distribution within each circuit feature. This is to be distinguished from the conventional approaches where multiple layers of different resists, e.g., a bilayer resist system, are employed in order to achieve certain types of sidewalls. That is, the goal is to realize a desired (target) sidewall on a homogeneous resist system by dose modulation only. In this article, a method which uses a 3D PSF in controlling e-beam dose in order to achieve a target remaining resist profile is described, and the simulation results from the proof-of-concept implementation of the method are presented. To the authors' knowledge, this is the very first attempt to develop a true 3D e-beam proximity effect correction scheme which utilizes 3D PSF's, while there were efforts to analyze 3D resist profiles.[8] The dose to be given to each region of a feature is determined such that the 3D remaining resist profile is as close to the target profile as possible. Through iterations, the dose distribution within each feature is adjusted so that the difference between the target and estimated profiles is minimized.

II. 3D MODELS

Conventional proximity effect correction schemes employ a 2D correction model where variation of exposure distribution along the resist depth dimension is not considered. In
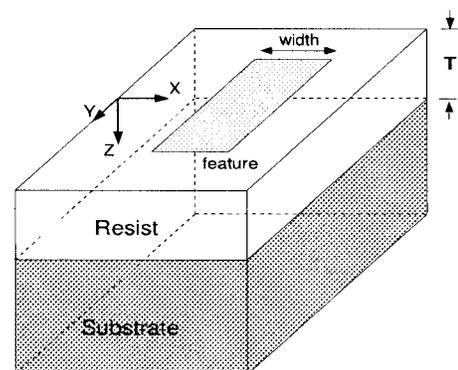

FIG. 1. 3D model where the *Z* axis represents the resist depth.

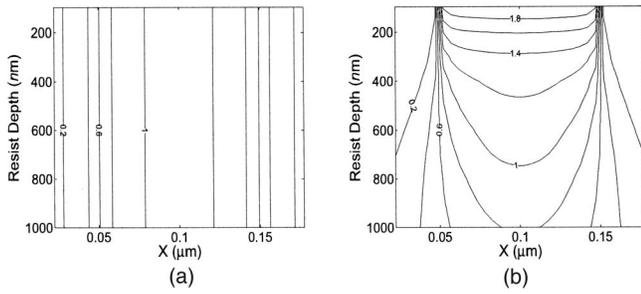[a)]Electronic mail: leesooy@eng.auburn.edu

FIG. 2. Exposure distribution in the cross section of a line feature, estimated by (a) 2D model and (b) 3D model, where the feature width is 100 nm, the resist (PMMA) thickness is 1000 nm, and the beam energy is 50 keV.

FIG. 3. Remaining resist profile for the line feature in Fig. 2 where the number on each curve indicates the respective developing time.

order to develop a true 3D correction scheme, 3D models for exposure and resist development are employed. Such 3D models allow the correction scheme to have a better control of the critical dimension (CD) and sidewall shape of each feature.

A. Exposure model

The substrate system consists of a substrate and a certain type of resist as illustrated in Fig. 1. It is assumed that the substrate and resist are spatially homogeneous, i.e., the substrate composition and the resist thickness do not change with location. A 3D point spread function is denoted by $PSF(x,y,z)$ which describes the exposure distribution in the resist when a point on the X-Y plane is exposed. The resist depth is along the Z axis. Let $f(x,y,0)$ represent the dose to be given to each point $(x,y,0)$ on the resist surface for writing a circuit pattern. For example, when each circuit feature is exposed with a constant dose D, then $f(x,y,0)=D$ if $(x,y,0)$ is within a feature [$f(x,y,0)=0$ otherwise]. Let us denote the exposure distribution in the resist by $e(x,y,z)$. Assuming that the e-beam lithographic process is linear and space invariant, $e(x,y,z)$ can be expressed by the following convolution:[7]

$$e(e,y,z) = \int_{x'} \int_{y'} \int_{z'} PSF(x-x',y-y',z-z')$$
$$\times f(x',y',0)dx'dy'dz'$$
$$= \int_{x'} \int_{y'} PSF(x-x',y-y',z)f(x',y')dx'dy'.$$

From this equation, it is seen that the exposure distribution at a certain depth (z_0) can be computed by the 2D convolution between $f(x,y,0)$ and $PSF(x,y,z_0)$ in the corresponding plane or *layer*, $z=z_0$. Modeling a homogeneous resist system as a stack of conceptual layers, $e(x,y,z)$ may be estimated layer by layer. In general, $e(x,y,z) \neq e(x,y,z')$ where $z \neq z'$. In Fig. 2, exposure distributions estimated by the 2D and 3D models are compared. It is clearly seen that exposure varies greatly along the resist depth dimension.
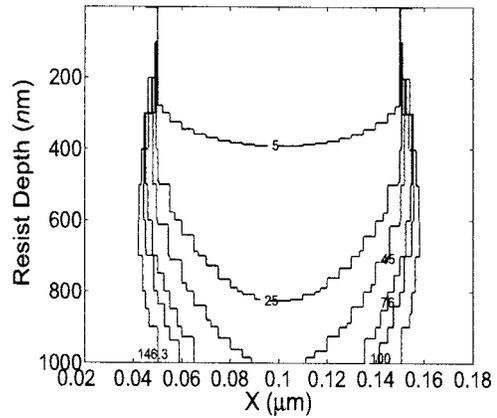
B. Development model

While the 3D exposure model provides complete information on how electron energy is distributed in the resist, it does not directly depict the remaining resist profile after development. In order to make correction results more realistic, one may take the resist development process into account for correction. Given a spatial exposure distribution in the resist, the remaining resist profile after development can be estimated through computer simulation. Then, the estimated profile is referred to in determining dose distribution.

In this study, a simplified version of the resist development model ("cell removal model"), PEACE,[8] is employed to demonstrate the effectiveness of the proposed approach to 3D correction. Only the cross sections of long features such as lines are considered since the main focus of this study is on controlling CD and sidewall shape. In the model, resist is partitioned into rectangular cells and exposure is estimated at each cell. The developing rate of each cell is computed from its exposure.[9] Through iterations, the remaining time for complete development of each of the exposed cells is updated, taking the number of its exposed sides into account. Simulation continues for a specified developing time, and then the remaining resist profile is obtained.

In Fig. 3, the remaining resist profile is plotted with the developing time varied for the exposure distribution in Fig. 2. It is observed that no remaining resist profile matches any isoexposure contour. That is, in order to minimize the real CD error, the remaining resist profile is to be used in correction instead of exposure distribution itself.
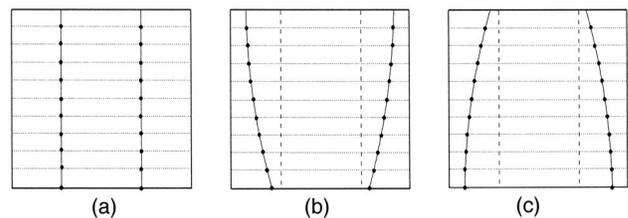

FIG. 4. Distribution of critical points for (a) vertical sidewall, (b) overcut, and (c) undercut.
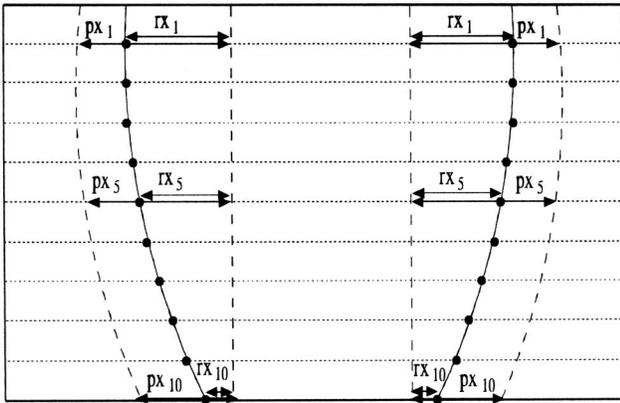
FIG. 5. Cost function is formulated as a combination of CD errors on all layers, i.e., $L(\{rx_i - px_i\})$ where rx_i and px_i are the target and actual widths measured from a reference point on the ith layer.

III. 2D CORRECTION

The proximity effect correction schemes developed so far employ a 2D PSF, $PSF(x,y)$, to estimate the 2D exposure distribution, $e(x,y)$, in the resist. That is,

$$e(x,y) = \int_{x'} \int_{y'} PSF(x - x', y - y')f(x',y')dx'dy'.$$

During correction, the dose distribution, $f(x,y)$, is determined such that $e(x,y)$ is as high as possible (or at least well above the developing threshold) within features and is as low as possible outside them. More specifically, in PYRAMID, each circuit feature is partitioned into regions and a set of *critical points* is set up along the boundaries of each circuit feature. The dose to be given to each region is determined based on the exposure estimate at the corresponding critical point through iterations. Note that the exposure estimated at each critical point is the one averaged along the resist depth dimension.

IV. 3D CORRECTION

In 3D correction, the 3D exposure distribution in the resist, $e(x,y,z)$, is referred to, as discussed in Sec. II A. The main idea of 3D correction is to control $e(x,y,z)$ such that the target remaining resist profile is obtained. If a feature is exposed with a single dose, controllability is limited. Note that changing the single dose merely scales up or down $e(x,y,z)$ with the spatial distribution of isoexposure contours fixed. Therefore, it is necessary to partition each feature so that dose can be varied within the feature in order to have a better control of $e(x,y,z)$. In this section, two proof-of-concept implementations of 3D correction are described, i.e., *isoexposure correction* and *resist profile correction*. The overall 3D correction procedure is built upon the correction hierarchy of PYRAMID.[10–12]
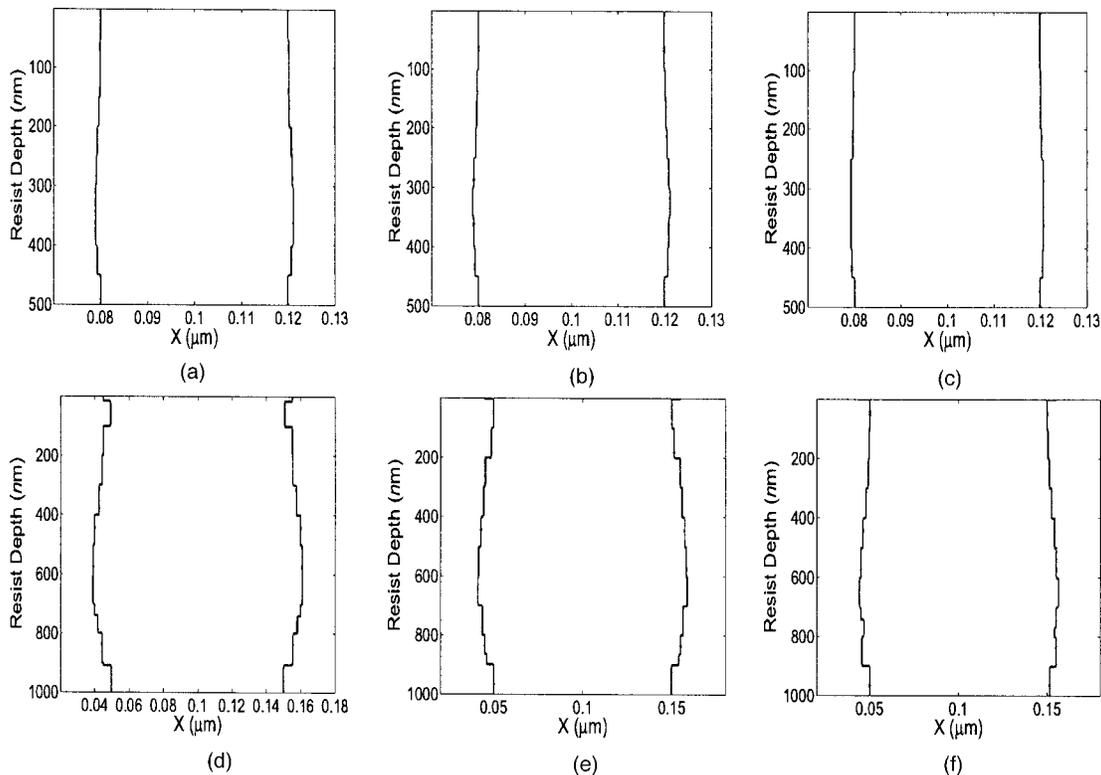

FIG. 6. Remaining resist profiles (vertical sidewalls) for linewidth of 40 nm (500 nm PMMA on Si, 50 keV), (a) 2D correction, (b) 3D isoexposure correction, and (c) 3D resist profile correction, and linewidth of 100 nm (1000 nm PMMA on Si, 50 keV), (d) 2D correction, (e) 3D isoexposure correction, and (f) 3D resist profile correction.
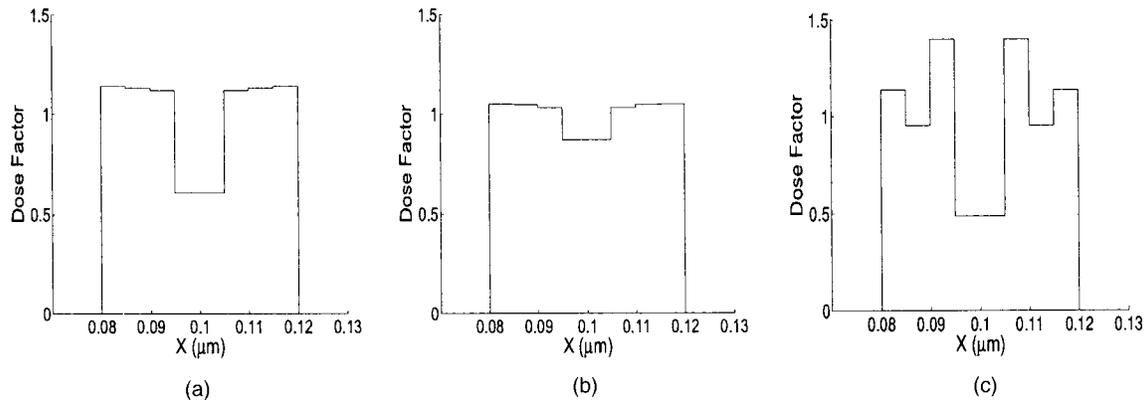
FIG. 7. Dose factor distribution obtained by (a) 2D correction, (b) 3D isoexposure correction, and (c) 3D resist profile correction for linewidth of 40 nm (500 nm PMMA on Si, 50 keV) in Fig. 6. The pixel size (interval) is 5 nm.

A. Isoexposure contour correction

In this correction, the exposure model described in Sec. II A is employed as in most of the proximity effect correction schemes developed so far. The goal of this correction scheme is to match an isoexposure contour to the shape of the sidewall that needs to be achieved. Let us consider a single line feature which is long enough for exposure variation along the length dimension to be negligible. A set of critical points is set up along the target sidewalls of the cross section as illustrated in Fig. 4. The line feature is partitioned into regions (along the length dimension), for each of which a dose is to be determined. Exposure at each critical point is estimated using the PSF at the corresponding layer. In determining the dose of each region, a set of critical points, one from each layer, is considered. Let d_i be the dose required for the region in order to achieve the target exposure (e.g., developing threshold) at the critical point in the ith layer. In general, $d_i \neq d_j$ for $i \neq j$. Therefore, the dose for the region may be set to a certain combination of $\{d_i\}$, e.g., $\Sigma w_i d_i$ where $\Sigma w_i = 1$, or more generally a value which minimizes a cost

FIG. 8. Remaining resist profiles (overcut) for linewidth of 100 nm (100 nm PMMA on Si, 50 keV), (a) 2D correction, (b) 3D isoexposure correction, and (c) 3D resist profile correction, and linewidth of 100 nm (500 nm PMMA on Si, 50 keV), (d) 2D correction, (e) 3D isoexposure correction, and (f) 3D resist profile correction.
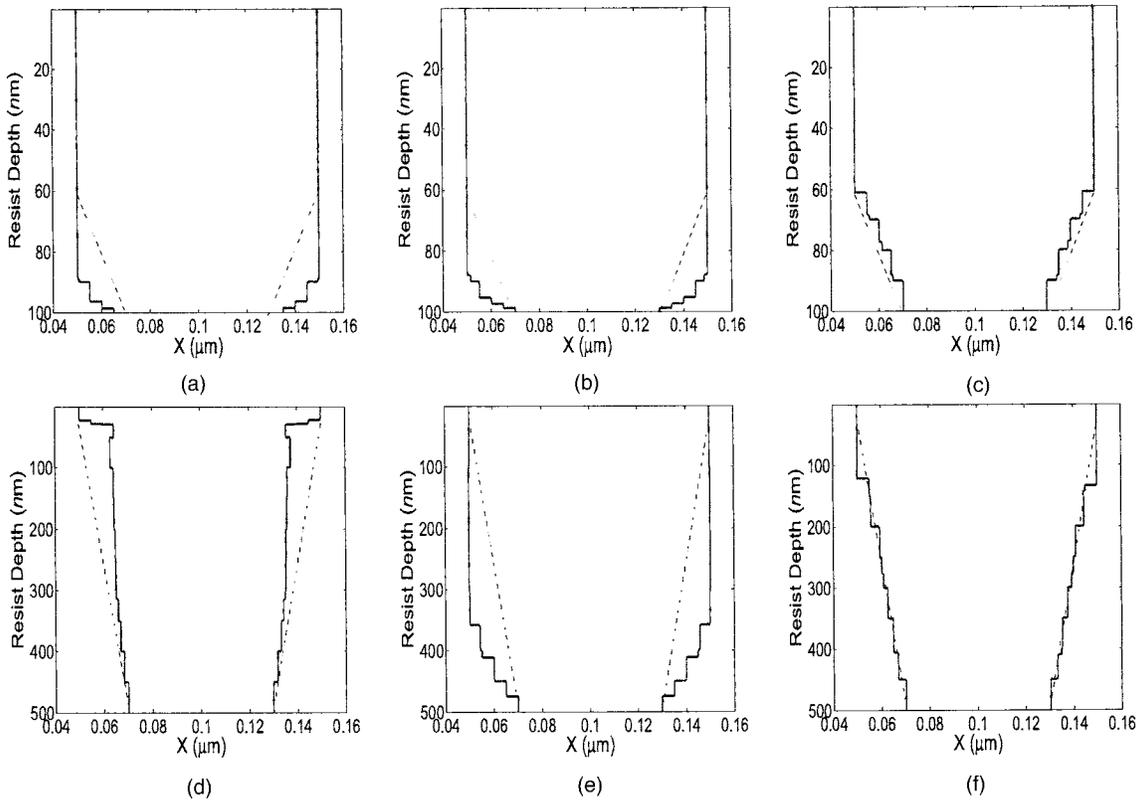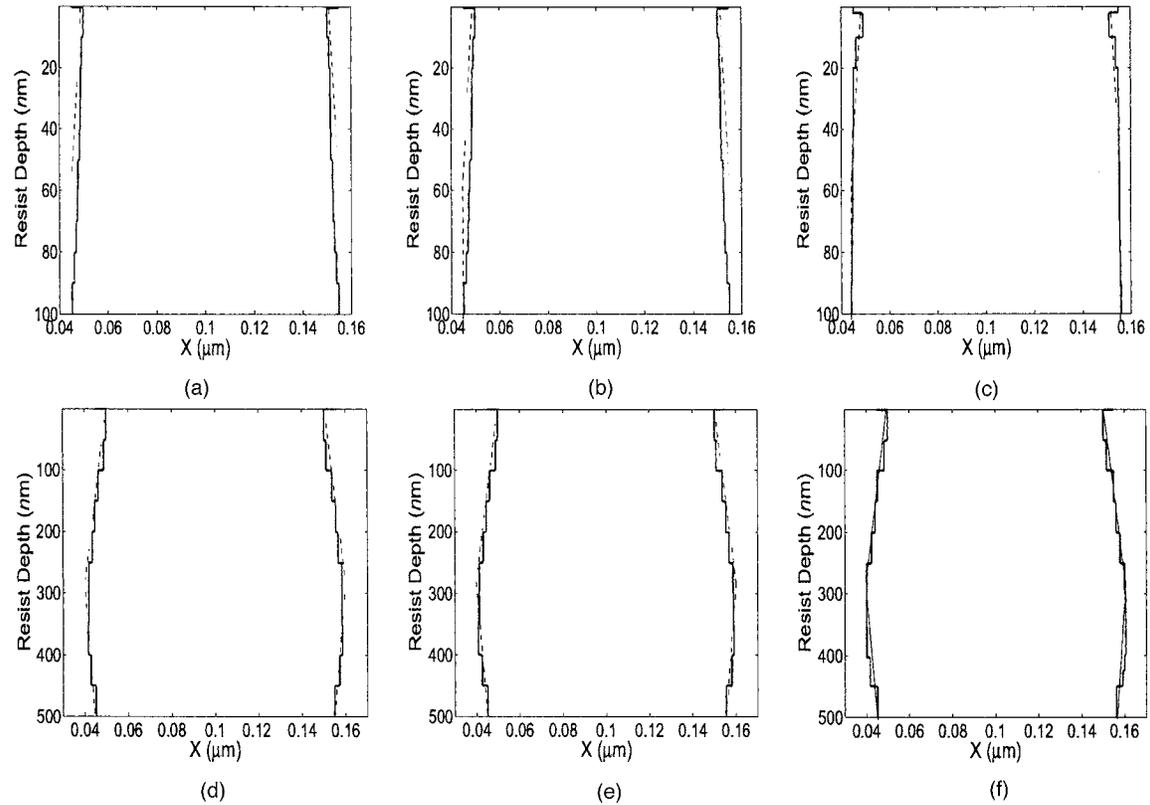
FIG. 9. Remaining resist profiles (undercut) for linewidth of 40 nm (100 nm PMMA on Si, 50 keV), (a) 2D correction, (b) 3D isoexposure correction, and (c) 3D resist profile correction, and linewidth of 100 nm (500 nm PMMA on Si, 20 keV), (d) 2D correction, (e) 3D isoexposure correction, and (f) 3D resist profile correction.

function of deviations from the target exposure at the critical points. Doses of all regions are adjusted through iterations such that the deviations of exposures at the critical points from the target exposure are minimized.

B. Resist profile correction

The main problem with the isoexposure correction is that a remaining resist profile does not correspond to any single isoexposure (refer to Sec. II B). Therefore, even if a dose distribution which results in an isoexposure contour matching a target remaining resist profile is found, the target remaining resist profile is unlikely to be obtained after development. In order to make correction results more realistic, the development model described in Sec. II B is employed instead of the exposure model. That is, the estimated remaining resist profile rather than an isoexposure contour is used as a reference for optimization during correction.

Again, consider a long line feature. Exposure, $e(x,z)$, in the cross section of the line is estimated, from which the resist developing rate, $r(x,z)$, is computed. Using the resist development model described in Sec. II B, the remaining resist profile is predicted through simulation. The CD error on each layer ($rx_i - px_i$ in Fig. 5) is computed, and a cost function is derived as a certain combination of the CD errors. Then, the dose of each region is determined such that the cost function is minimized. Doses of all regions are adjusted through iterations until a termination condition is met.

V. SIMULATION RESULTS AND DISCUSSION

In order to demonstrate the improved control of sidewall shape by 3D correction, an extensive simulation has been carried out by implementing a proof-of-concept design of the proposed true 3D correction scheme. The two versions of 3D correction described in Sec. IV have been implemented, which are compared to the 2D correction (refer to Sec. III). In Fig. 6, some of the simulation results for vertical sidewall are provided, where the remaining resist profiles of a single line are compared. It is clearly seen that the resist profiles achieved by the 3D resist profile correction are significantly better than those by the 2D or 3D isoexposure correction. The CD errors for the 3D resist profile correction are much smaller than those for the 2D correction. It is also observed that a thicker resist leads to larger CD errors as expected since exposure variation along the resist depth dimension is larger. In Fig. 7, the dose factors (dose normalized by the base dose) distribution obtained by the three correction schemes are shown, which result in the remaining resist profiles in Figs. 6(a)–6(c). It is noted that the dose distribution by the resist profile correction is significantly different from those by the other two corrections.

In Fig. 8, two sets of the remaining resist profiles are provided. In each set, a certain overcut sidewall, indicated by the dashed lines, was to be obtained. In the 2D correction results, it can be seen that the CD specification is well matched at the top and bottom layers, but there are signifi-
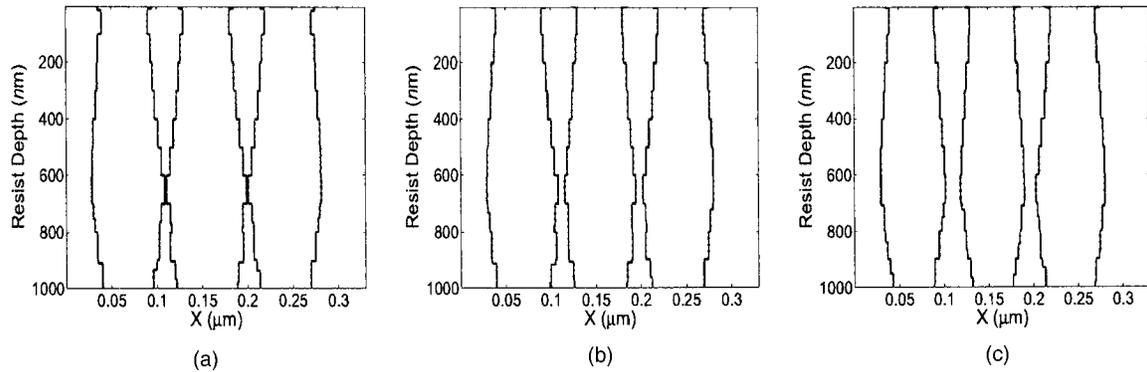
FIG. 10. Remaining resist profiles for a three-line pattern ($L/S=50/40$ nm, 1000 nm PMMA on Si, 50 keV), (a) 2D correction, (b) 3D isoexposure correction, and (c) 3D resist profile correction.

cant CD errors in most of the layers between them. No significant improvement has been achieved by the 3D isoexposure correction. However, the remaining resist profiles obtained by the 3D resist profile correction are much closer to the target profiles.

In Fig. 9, simulation results for undercuts are presented. The target undercut profiles are indicated by the dashed lines. In these results, the improvement by the 3D resist profile correction is not so significant as in the other two types of sidewalls. Note that the 2D results do not have large CD errors. Nevertheless, one can notice a substantial difference between the target and actual profiles in the middle layers in the cases of the 2D and 3D isoexposure correction results while there is no such difference in the 3D resist profile correction results.

In Fig. 10, the remaining resist profiles of a three-line pattern corrected for 1000 nm polymethyl methacrylate (PMMA) on Si (50 keV) are shown, where vertical sidewalls are to be achieved. The linewidth is 50 nm and the space between lines is 40 nm. The 2D correction result shows a significant interproximity effect in the middle layers where the lines are almost merged. However, the result by the 3D resist profile correction exhibits substantially less interproximity effect, and the sidewalls are more vertical than those obtained by the 2D and 3D isoexposure corrections. Controlling sidewall shape can also help improve resolution or feature density especially in the case of vertical sidewall. Note that features can be placed closer to each other when sidewalls are more vertical.

VI. SUMMARY

The proximity effect correction schemes developed so far employ a 2D PSF, i.e., no consideration of exposure variation along the resist depth dimension. However, it is often desirable or necessary to have an explicit control of 3D exposure distribution in the resist in order to achieve high dimensional accuracy of the developed features. This is particularly so when the degree of 3D proximity effect[7] is high. In this article, an approach to true 3D proximity effect correction and its proof-of-concept implementation are de-

scribed. Instead of exposure itself, the 3D remaining resist profile is used as a reference for optimization during correction. Dose to be given to each region is determined iteratively such that deviation from the target remaining resist profile is minimized. While the potential benefit of the proposed 3D proximity effect correction in minimizing CD errors and controlling sidewall shape has been demonstrated through simulation, generalization of the implementation and improvement of the optimization procedure are ongoing efforts. Note that what is proposed in this article is an attempt to control 3D exposure distribution in the resist by 2D dose distribution on the top of the resist. Therefore, controllability of the 3D distribution of exposure is limited, hence making the proposed 3D correction challenging. Also, one practical drawback of the current implementation is its increased computation time (in the order of 10–100 times longer) mainly due to the resist development simulation and, therefore, a fast yet accurate method for the simulation will need to be developed in order to make this true 3D correction applicable to circuit patterns of realistic size.

ACKNOWLEDGMENT

[1]M. Parikh, IBM Tech. Discl. Bull. **22**, 5187 (1980).
[2]D. P. Kern, *Proceedings of the Ninth International Conference on Electron and Ion Beam Science and Technology*, edited by R. Bakish (Electrochemical Society, Princeton, NJ, 1980), p. 326–339.
[3]E. Kratschmer, J. Vac. Sci. Technol. **19**, 1264 (1981).
[4]G. Owen, J. Vac. Sci. Technol. B **8**, 1889 (1990).
[5]S.-Y. Lee, J. C. Jacob, C. M. Chen, J. A. McMillan, and N. C. MacDonald, J. Vac. Sci. Technol. B **9**, 3048 (1991).
[6]U. Hofmann, C. Kalus, A. Rosenbusch, R. Jonckheere, and A. Hourd, Proc. SPIE **2723**, 150 (1996).
[7]S.-Y. Lee and Kasi Anbumony, Microelectron. Eng. **83**, 336 (2006).
[8]Y. Hirai, S. Tomida, K. Ikeda, M. Sasago, M. Endo, S. Hayama, and N. Nomura, IEEE Trans. Comput.-Aided Des. **16**, 802 (1991).
[9]D. Kyser and N. Viswanathan, J. Vac. Sci. Technol. **12**, 1305 (1975).
[10]B. D. Cook and S.-Y. Lee, IEEE Trans. Semicond. Manuf. **11**, 117 (1998).
[11]S.-Y. Lee and D. He, Microelectron. Eng. **69**, 47 (2003).
[12]F. Hu and S.-Y. Lee, J. Vac. Sci. Technol. B **21**, 2672 (2003).